

Thickness of a three-sided coin: A molecular dynamics studyGopinath Subramanian *X-Computational Physics Division, Los Alamos National Laboratory, Los Alamos, New Mexico 87545, USA*

(Received 30 December 2020; accepted 5 April 2021; published 26 April 2021)

This Letter presents a numerical study across parameter space to calculate the aspect ratio (ratio of length to diameter) of a fair “three-sided coin”: a cylinder that when tossed, has equal probabilities of landing heads, tails, or sideways. The results are cast in the context of previous analytical studies, and the various mechanisms that govern the dynamics of coin tossing are compared and contrasted. After more than 7×10^8 tosses of coins of various aspect ratios, this study finds the critical aspect ratio to be slightly less than (but not exactly equal to) $\sqrt{3}/2 \approx 0.866$.

DOI: [10.1103/PhysRevE.103.L041301](https://doi.org/10.1103/PhysRevE.103.L041301)**I. INTRODUCTION**

In systems whose evolution is governed by deterministic Newtonian mechanics, slight variations in initial conditions combined with a long evolution time may render the system chaotic. The final outcome of such systems is effectively random and necessitates a probabilistic treatment. The first studies of problems involving chance can be attributed to Cardano [1], whose studies of dice, cards, and knucklebones laid the foundations for the theory of probability. One of the simplest systems that exhibits effectively random behavior is a tossed coin, and the first step in incorporating probability into the physics of a tossed coin (by choosing an initial angular velocity drawn from a distribution) was taken by Keller [2], who examined the tossing of a coin of zero thickness. Other more sophisticated models for a coin with finite thickness were developed by Vulović and Prange [3], Bondi [4], Kuindersma and Blais [5], and Yong and Mahadevan [6], some of which have accounted for bouncing of the coin in various ways, precession of the coin, and for scenarios where the coin falls on a perfectly inelastic surface.

The problem of tossing a thick coin was recently popularized by Parker and Hunt’s video titled “How thick is a three-sided coin?” on the popular website YouTube [7]. Parker and Hunt view coins as cylinders, and seek to determine the critical value of the aspect ratio that results in a coin having a probability of landing either heads, tails, or sides, each equal to 1/3. As with some previous studies, the authors used a model based on the ratios of areas to calculate a critical aspect ratio.

As with most complex dynamical systems described by differential equations, numerical methods can be used to minimize the number of assumptions that simpler models adopt. Numerical methods have the additional advantage that reliable statistics can be gathered over a range of initial conditions and parameters. In this study, we report the statistics of tossing a coin of various aspect ratios obtained using the molecular dynamics (MD) method. MD been used for numerous atomistic and coarse grained studies to examine phenomena as diverse as ion diffusion [8], radiation damage evolution [9], and the

thermodynamics of DNA and RNA [10]. In the remainder of the Letter, we briefly describe our protocol for constructing a coin and tossing it, and present our results. We find Bondi’s model [4] to be the most realistic, as it incorporates the physics of a coin falling on a surface, losing energy, and then rolling over.

II. METHODS

We consider coins to be cylinders of diameter D and length (or thickness) L . As is common in the fluid mechanics [11] and materials science [12] communities, we use the definition of aspect ratio of the cylinder $\phi = L/D$. All coins in this study are then discretized into a set of spheres of diameter d , shown schematically in Fig. 1, where hard spheres are placed along the circumference of the circular faces of the cylinder. In this schematic, 30 hard spheres are used to discretize the cylinder. The actual range of the number of spheres used for the discretization, along with a discussion of roughness, is presented later in this Letter.

All spheres that make up the coin are constrained to remain stationary with respect to each other, thereby constraining the coin to move (translate + rotate) as a rigid body. All spheres are assigned a mass m , and interact with the x - y plane at $z = 0$ with a shifted and truncated (purely repulsive) Lennard-Jones potential,

$$U_{LJ}(z) = \begin{cases} \varepsilon + 4\varepsilon[(\sigma/z)^{12} - (\sigma/z)^6] & z \leq z_c \\ 0 & z > z_c. \end{cases} \quad (1)$$

The quantities σ and ε set the length and timescales of the simulations. The fundamental units of mass, length, and time are, respectively, m , σ , and $\tau = \sigma(m/\varepsilon)^{1/2}$. The cutoff distance is chosen as $z_c = 2^{1/6}\sigma$, making the potential purely repulsive. The addition of ε ensures that $U_{LJ}(z_c) = 0$, and eliminates the discontinuity at the energy minimum. Moreover, this cutoff distance is also equal to the diameter of each Lennard-Jones sphere, d . During the discretization, all spheres are placed such that the center-to-center distance of

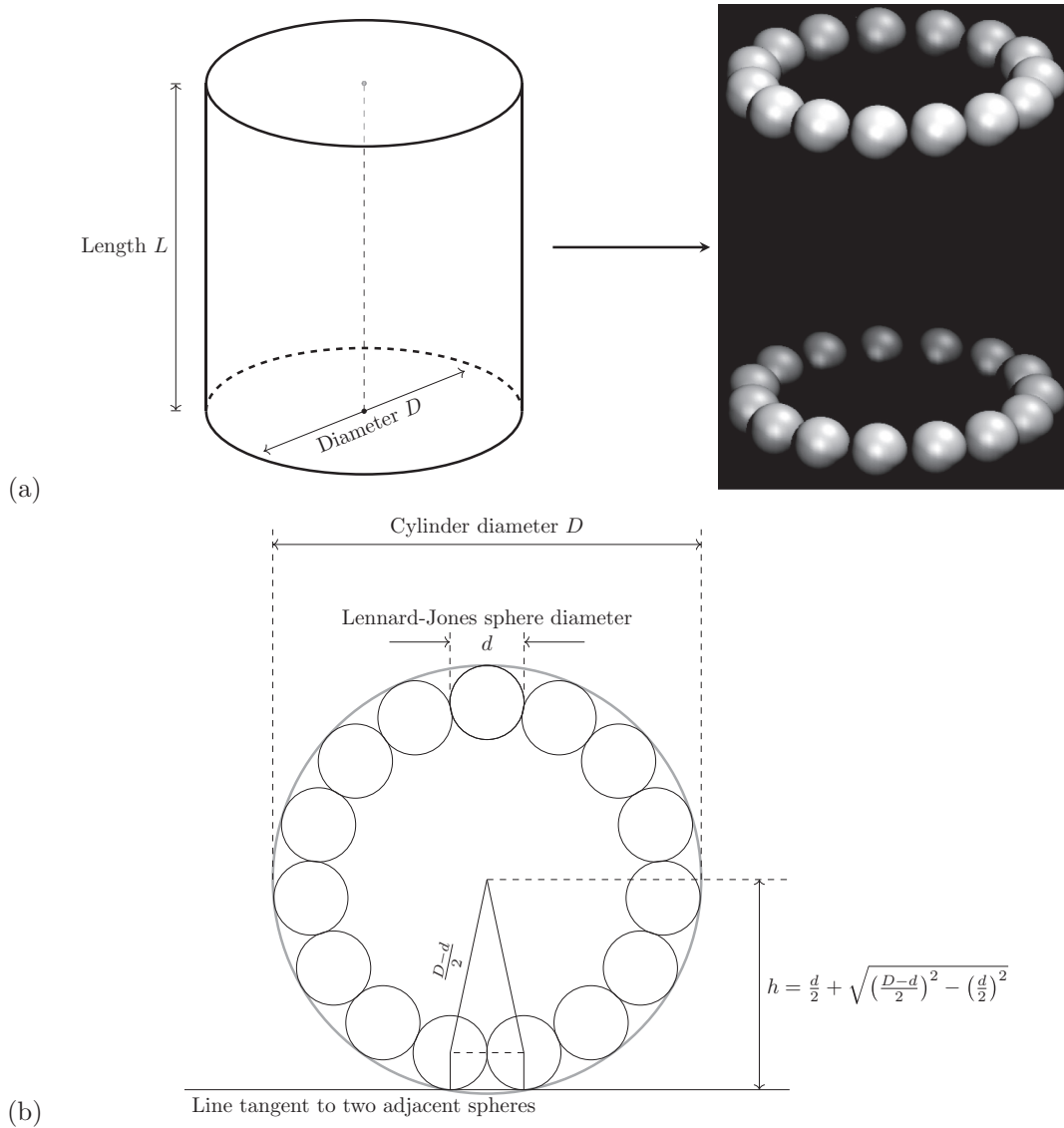


FIG. 1. Schematic of the discretization used in this study. We use the definition of aspect ratio $\phi = L/D$. In this model, the diameter of each Lennard-Jones sphere is $d = 2^{1/6}\sigma$, which is also the center-to-center distance (along a straight line, not the circumference) of adjacent spheres. (a) Discretization of an ideal cylinder into spheres. (b) View along the cylinder axis. Here, h is the height of the cylinder axis above a horizontal plane when the cylinder is in equilibrium, and is used as a measure of cylinder roughness.

adjacent spheres (along a straight line, not the circumference) is also equal to d .

As a result of this discretization, the cylinder surface is not smooth. When the cylinder is in equilibrium on the x - y plane, the height of the cylinder axis above this plane is h , and is slightly lower than the ideal height $D/2$. The quantity h can be obtained from the geometry shown in Fig. 1(b), and the ratio $2h/D$ is used as a measure of deviation from an ideal cylinder surface.

All spheres in the simulation are also subjected to a gravitational potential that mimics an acceleration due to gravity of g :

$$U_g(z) = mgz. \tag{2}$$

Each coin was then “tossed” using the following protocol:

(1) Place the coin with its centroid at the origin. Rotate the axis of the cylinder about the y axis by an angle θ uniformly

distributed between $[0, \pi/2]$, and raise the centroid of the coin to a height H . This method of choosing the initial position is sufficient to include all possible initial positions due to the symmetry of the problem.

(2) The spheres that make up the coin are assigned an initial velocity, such that the coin as a whole has an angular velocity ω uniformly distributed between $[0, \omega_{\max}]$. This angular velocity is imparted about an axis of rotation perpendicular to the cylinder axis and passing through the centroid, thereby emulating the tossing of a coin. No rotation about the cylinder axis is imparted, as this would undesirably stabilize the coin.

(3) The equations of motion are then integrated for a randomization time t_{rand} . Note that during this (and other) time integrations, the spheres making up the coin are constrained to move as a rigid body.

(4) After randomization, a viscous damping force $F = -kv$ (where v is the velocity of a sphere) is introduced

TABLE I. Summary of the parameters used in this study. The diameter of a Lennard-Jones sphere in this model is $d = 2^{1/6}\sigma$.

Parameter	Value
Acceleration due to gravity g	$2\sigma\tau^{-2}$
Initial height H	10x the largest dimension of the coin
Maximum angular velocity of rotation ω_{\max}	$10 \times 2\pi / \sqrt{2gh}$
Time step Δt	$10^{-3}\tau$
Randomization time t_{rand}	$10^5\Delta t$
Viscous damping coefficient k	0.1
Smallest external diameter	2.909σ (5 spheres along the circumference)
Largest external diameter	18.987σ (50 spheres along the circumference)
Smallest thickness	$2 \times d = 2.245\sigma$
Largest thickness	$20 \times d = 22.449\sigma$

to the equations of motion to slowly drain the kinetic energy of the coin.

(5) The equations of motion are integrated until the coin's velocity becomes negligibly small.

(6) The direction of the cylinder axis is noted and used to decide whether the coin landed heads, tails, or sideways.

The LAMMPS molecular dynamics package [13] was used for all simulations. This coin toss experiment was repeated a large number of times to gather statistics.

III. RESULTS AND DISCUSSION

Table I summarizes the various parameters used in this study, along with the range of coin sizes. This combination of parameters, chosen by trial and error, allows the coin to bounce at least twice during the randomization phase and that for typical initial conditions, performs ≈ 5 rotations before the first bounce. We believe that these choices are sufficient to allow the coin toss to be effectively random.

The aspect ratio ϕ of the coin is defined as the ratio of the length of the cylinder axis to its diameter. For each aspect ratio, the coin was tossed 8.74×10^5 times using the protocol described above. The statistics obtained are plotted in Fig. 2, which shows the probability of obtaining heads,

tails, and sideways (denoted by P_h , P_t , and P_s , respectively) as a function of the coin's aspect ratio. In this plot, there is a fourth set of data obtained from small diameter coins. We have plotted P_h , P_t , and P_s using a single symbol (open squares) for these coins, as these data suffer from artifacts arising from the discretization.

Coins with $D \leq 7.196$ (corresponding to 17 or fewer Lennard-Jones spheres along the circumference of one face, or 34 spheres in total) were categorized as small diameter. This cutoff corresponds to the ratio $2h/D = 0.996$. The choice of this cutoff, while arbitrary, appears to allow the "good" data to fall on sigmoidal trendlines. Furthermore, we see that data from the small diameter coins deviates from the trendlines only at moderate aspect ratios between, say, 0.8 and 1.5.

Focusing on the data that do not seem to suffer from discretization artifacts, we see that in the limit that $\phi \rightarrow 0$, which represents a very thin coin, we obtain the classically expected result of $P_h = P_t = 0.5$, and $P_s = 0$. As we increase the thickness of the coin, we start to see significant deviations from the behavior of a fair coin at $\phi \approx 0.5$, where the probability of the coin landing on its side is non-negligible. The thick coin limit seems to be attained at $\phi \approx 2.5$, where the probability of obtaining heads or tails is practically zero, and we are approaching the expected behavior of the limit $\phi \rightarrow \infty$.

At a critical aspect ratio close to (but not exactly equal to) $\phi_c \approx \sqrt{3}/2 \approx 0.866$, we see that the three probabilities are nearly equal. This critical aspect ratio is markedly different from the results of previous, more simplistic studies. We believe that this is because our numerical study incorporates many of the dynamical subtleties that can be difficult to incorporate in simpler analytical treatments. For example, Yong and Mahadevan [6] obtained $\phi_c = 0.577$ with the assumption that the coins land on a "jellylike" surface, i.e., when a coin hits the surface, it immediately ceases all motion. Parker and Hunt, using the ratios of projected areas, calculate $\phi_c = 1/\sqrt{3}$ [7].

Of the many models present in the literature, Bondi's model [4], which used energy considerations on a perfectly inelastic surface to determine that $\phi_c = 0.75$, comes closest to the value presented in this work, and is thus discussed in more detail. Bondi assumes that when the cylinder hits the ground, it completely loses all kinetic energy. However, since the centroid of the cylinder is higher than the equilibrium position, it then continues to roll until the next impact, and so on until it comes to rest. Since Bondi's notation is different

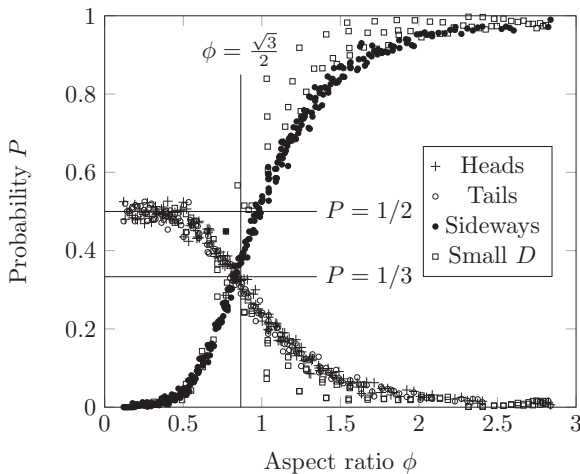


FIG. 2. Results of coin tosses for various aspect ratios. We have used the definition of aspect ratio as the ratio of the length to diameter of the cylinder, i.e., $\phi = L/D$.

from that used in this Letter, the steps taken to translate the results from his notation to ours are outlined next. He defines the length of a “diagonal” $2f$, and an angle σ between the axis of the cylinder and its diagonal, such that the diameter of the cylinder is $D = 2f \sin \sigma$ and the length of the cylinder is $L = 2f \cos \sigma$. He then proceeds to determine that the “side trap” has a width of $f(1 - \sin \sigma)$ and the “base trap” has a width of $f(1 - \cos \sigma)$, and the ratio of probabilities ending up on the base (either heads or tails) or on the side is the ratio

of these trap widths. Thus, for $P_h = P_t = P_s = 1/3$, we obtain $\phi_c = 0.75$, which is closer to our value. Bondi then goes on to describe how his analysis could be extended to imperfectly inelastic collisions, but does not follow through. The results of the present study indicate that an extension of Bondi’s model might yield an analytical solution.

ACKNOWLEDGMENT

This Letter has been designated No. LA-UR-20-30039.

-
- [1] G. Cardano, *Liber De Ludo Aleae (The Book on Games of Chance)* (1663).
 - [2] J. B. Keller, The probability of heads, *Am. Math. Month.* **93**, 191 (1986).
 - [3] V. Z. Vulović and Richard E. Prange, Randomness of a true coin toss, *Phys. Rev. A* **33**, 576 (1986).
 - [4] S. H. Bondi, The dropping of a cylinder, *Eur. J. Phys.* **14**, 136 (1993).
 - [5] S. R. Kuindersma and B. S. Blais, Teaching Bayesian model comparison with the three-sided coin, *Am. Stat.* **61**, 239 (2007).
 - [6] E. H. Yong and L. Mahadevan, Probability, geometry, and dynamics in the toss of a thick coin, *Am. J. Phys.* **79**, 1195 (2011).
 - [7] M. Parker and H. Hunt, How thick is a three-sided coin? (2018), <https://youtu.be/-qqPKKOU-yY>.
 - [8] T. J. Yoon, L. A. Patel, M. J. Vigil, K. A. Maerzke, A. T. Findikoglu, and R. P. Currier, Electrical conductivity, ion pairing, and ion self-diffusion in aqueous NaCl solutions at elevated temperatures and pressures, *J. Chem. Phys.* **151**, 224504 (2019).
 - [9] B. P. Uberuaga, E. Martínez, D. Perez, and A. F. Voter, Discovering mechanisms relevant for radiation damage evolution, *Comput. Mater. Sci.* **147**, 282 (2018).
 - [10] A. Prhashanna and A. Jayaraman, Melting thermodynamics of oligonucleic acids conjugated with relatively solvophobic linear polymers: A coarse-grained molecular simulation study, *J. Polymer Sci. Part B: Polymer Phys.* **57**, 1196 (2019).
 - [11] S. Dutta, M. J. Andrews, and J.-C. Han, Turbulent flow and heat transfer in rotating different aspect ratio channels, *J. Thermophys. Heat Trans.* **11**, 318 (1997).
 - [12] L. Chen, R. Ozisik, and L. S. Schadler, The influence of carbon nanotube aspect ratio on the foam morphology of MWNT/PMMA nanocomposite foams, *Polymer* **51**, 2368 (2010).
 - [13] S. Plimpton, Fast parallel algorithms for short-range molecular dynamics, *J. Comput. Phys.* **117**, 1 (1995).